Multiomic characterisation of high grade serous carcinoma enables high resolution patient stratification

Hollis et al.

SUPPLEMENTARY INFORMATION

SUPPLEMENTARY METHODS

1. Pathology review and immunohistochemistry for WT1 and p53

H&E-stained slides underwent pathology review by two expert gynaecological pathologists (ARWW, WGM) prior to the initial transcriptomic characterisation of these samples (1,2). Prior to inclusion in the matched genomic-transcriptomic HGSOC study, cases were subject to additional pathology review (CSH); cases uncertain to represent HGSOC (n=26) underwent IHC for WT1 and p53 to aid histotyping (HGSOC: WT1 positive, p53 aberrant expression pattern) (Figure S1).

WT1 and p53 IHC was performed on the Leica BOND III Autostainer using IHC protocol F with 1:1000 anti-WT1 6F-H2 antibody (DAKO) or 1:50 anti-p53 DO-7 antibody (DAKO). For WT1, positive staining was defined as positive tumour nuclei; negative staining was defined as no tumour nuclear staining with corresponding positive stromal cells. For p53, aberrant positive diffuse tumour nuclear staining or complete absence of tumour nuclear staining was defined as aberrant expression (3); variable nuclear intensity was defined as wild-type pattern. Stromal cells served as an internal positive control for both markers.

2. CCNE1 and EMSY copy number assays

CCNE1 and *EMSY* copy number (CN) were quantified by TaqMan qPCR Copy Number Assays (Hs07158517_cn and Hs06316346_cn, ThermoFisher Scientific) using the StepOne Plus Real-Time PCR System (Applied Biosystems, ThermoFisher Scientific) and StepOne Software Version 2.3 with 10ng

template DNA as determined by HS qubit assay. RNaseP reference assay was used as a copy number reference assay. NA12878 human reference DNA was purchased from the Coriell Institute and included in each run. CN variants were called with CopyCaller v2.0 software using NA12878 as a calibrator sample (CN=2).

CCNE1 copy number gain (*CCNE1*g) was defined as ≥4 *CCNE1* copies. *EMSY* amplification was defined as ≥6 copies of *EMSY*. FUOV1 and OVCAR3 cell line DNA samples were included as controls for gain of *CCNE1* and *EMSY*, respectively.

3. Custom Integrated DNA Technologies Gene Capture Panel

High throughput sequencing was performed using a custom Integrated DNA Technologies (IDT) gene capture panel with unique molecular indices (UMIs). Whole genome libraries were generated and pooled for target capture. The gene target panel was designed to capture all exonic regions of: *ABCB1*, *AC004223.3*, *ARID1A*, *ATM*, *ATR*, *ATRX*, *BAP1*, *BARD1*, *BCL2L1*, *BLM*, *BRAF*, *BRCA1*, *BRCA2*, *BRIP1*, *C11orf65*, *CCNE1*, *CDK12*, *CHD4*, *CHEK1*, *CHEK2*, *CTNNB1*, *EGFR*, *EMSY*, *ERBB2*, *ERCC4*, *EZH2*, *FANCA*, *FANCB*, *FANCC*, *FANCD2*, *FANCE*, *FANCF*, *FANCG*, *FANCI*, *FANCL*, *FANCM*, *GNAS*, *KIT*, *KRAS*, *MAD2L2*, *MDM2*, *MLH1*, *MRE11*, *MSH2*, *MSH6*, *MUS81*, *MUTYH*, *NBN*, *NDUFB2*, *NF1*, *NF2*, *NRAS*, *PALB2*, *PARP1*, *PARP2*, *PAXIP1*, *PDGFRA*, *PER3*, *PIK3CA*, *PMS2*, *PPP2R1A*, *PPP2R2A*, *PRKDC*, *PTEN*, *RAD50*, *RAD51*, *RAD51B*, *RAD51C*, *RAD54L*, *RB1*, *RNASEH2A*, *RNASEH2B*, *RNASEH2C*, *RPA1*, *RUNDC3B*, *SHFM1*, *SLC25A40*, *SLFN11*, *SLX4*, *TOE1*, *TP53*, *TP53BP1*, *UBE2T*, *VRK2*. Whole genome libraries were generated using 200ng input DNA and pooled into groups of 16 for target gene capture and sequencing using an Illumina NextSeq 550 at the Edinburgh Clinical Research Facility, Western General Hospital, Edinburgh, UK. The median per-sample mean target coverage was 593X (range 205-3278X).

4. Processing of sequencing data and variant calling

Sequence reads were processed using the bcbio v1.0.6 high throughput sequence analysis pipeline: reads were aligned to hg38 with bwa v0.7.17, sorted and duplicates marked with bamsormadup (biobambam v2.0.79), UMIs were added as tags with umis v0.9.0b0, files were converted to BAM format and indexed using samtools v1.6. Reads were then grouped by UMI, and consensus reads were called and filtered with fgbio v0.4.0. Consensus reads were extracted with bamtofastq (biobambam) and re-aligned, sorted and indexed. The aligned consensus reads underwent base quality score recalibration with the Genome Analysis Toolkit (GATK) v3.8 and variant calling was performed using a majority vote system from three variant callers (Freebayes v1.1.0.46 (4), VarDict Java v1.5.1 (5), and GATK Mutect2 (6)). The DKFZ bias filter was applied to identify likely false positive variants caused by strand bias or FFPE-induced DNA damage. Owing to the reported ubiquitous p53 disruption in HGSOC, *TP53* wild-type cases underwent manual review of aligned reads in IGV to confirm wild-type status; 24 further mutations were identified by manual review, the vast majority of which (n=20) were splice site mutations toward read ends.

5. Filtering of called variants

Called variants at a minimum 10% allele frequency were annotated using the Ensembl VEP v90.9 against Ensembl release 90 and filtered using VEP annotation and the ClinVar database (7) to retain only likely functional variation: variants documented as pathogenic were retained as mutations, and those documented as benign were filtered. Within the remaining callset, nonsense mutations, frameshifting indels and splice site variants were retained as likely detrimental variants. Remaining synonymous, missense non-coding and undocumented significance variants were filtered as variants of uncertain significance.

6. Transcriptomic characterisation and subtyping

Gene expression data were generated as part of a previous study identifying transcriptionally-defined molecular subtypes of HGSOC (1,2). Samples were characterised in a larger training cohort (n=247 HGSOC in the present study), and a subsequent validation cohort (n=115 HGSOC in the present study). RNA was extracted from macrodissected FFPE tumor material using the Roche High Pure FFPE RNA Isolation kit, cDNA was amplified using the NuGEN FFPE WT-Ovation FFPE System kit, then fragmented and labelled using the NuGEN Encore Biotin Module. Resultant products were hybridisation to the Ovarian DSA™ cDNA microarray platform. Each cohort was pre-processed using the Robust Multi-Array Average (RMA) method prior to a quality control.

TCGA- and Tothill-based transcriptomic subtypes were determined using the ConsensusOv R package (8) with the 'ConsensusOv' and 'Helland' approaches.

EMSY overexpression was defined as expression within the top 14% of cases, as indicated recommended by the previous *EMSY* expression study (2) (status already available for the training cases from the previous study, and determined for the validation cases accordingly).

7. Immune cell infiltration analysis

Tumour infiltrating CD3-positive and CD8-positive immune cells were quantified by immunohistochemistry of tumour tissue microarrays (TMAs); three 0.8mm cores were taken from a tumour-containing FFPE tumour block per patient to construct the HGSOC cohort TMA. 4um TMA sections were stained for CD3 and CD8 using the Leica BOND III Autostainer and Leica BOND ready-to-use anti-CD3 and anti-CD8 antibodies with IHC protocol F. Stained sections were imaged and analysed using QuPath version 0.1.2. Tumour area was marked as a region of interest and positive and negative cells were counted using the positive cell detection protocol. Where cases were unevaluable due to damaged/missing cores (n=24 for CD8, n=24 for CD3), whole slide 4um FFPE sections were stained for CD3 and CD8 where available (n=21 for CD8, n=21 for CD3) and virtual TMAs were constructed using

random sampling of 3 tumour-containing regions equivalent to the area of triplicate TMA cores. These were then analysed as above.

Automated positive cell quantification was validated by manual scoring of a subset of tumour-containing cores by two human observers (RLH, AHP) (180 randomly selected cores per marker), demonstrating excellent correlation between human and machine scoring (spearman's rho>0.95, P<0.0001 for both observers against QuPath).

Positive infiltrating cell burden was quantified as the percentage of positive cells within tumour islets.

8. Immunohistochemistry for PTEN and RB

PTEN and RB protein loss was detected by IHC using sections of the HGSOC TMA. PTEN IHC used 1:50 M3627 clone 6H2.1 (DAKO); RB IHC used 1:100 NCL-L-RB-358 (Leica). Loss was defined as complete loss of positive staining in tumour cells with positive adjacent stromal staining. Wild-type pattern was defined as positive tumour cell staining. Two observers scored each core independently (RLH, YI). Disagreement was resolved by subsequent discussion to reach a consensus call; where a consensus was not agreed, staining was regarded as non-evaluable.

Where cases were unevaluable due to damaged/missing cores or equivocal staining (n=33 for PTEN, n=44 for RB), whole slide 4µm FFPE sections were stained for PTEN and RB where available (n=21 for PTEN, n=34 for RB) and scored as above.

9.Copy number analysis from off-target sequencing reads

Aligned bam files produced by the bcbio nextgen workflow were used for further CN analysis. Relative CN for 50kB segments of the genome were determine using the CopywriteR R package (9), whereby off-target reads are used to produce genome-wide CN estimates.

CN loss events were defined as regions with a log2 CN ratio of ≤ -2; CN gain events were defined as regions with a log2 CN ratio of ≥1.5. For estimating CN of *RB1* and *PTEN*, the mean CN across the 50kB segments encompassing *RB1* and *PTEN* were calculated as the overall gene CN. For quantification of

total CN gains, adjacent 50kB segments that demonstrated CN gain were merged to be counted as a single large CN gain events (using a 10% tolerance for the CN gain threshold in adjacent segments). The same approach was applied when quantifying the total number of loss events.

Detection of structural variants such as translocations and inversions was not possible due to the need for split read coverage and high sequencing depth across breakpoints which are typically intronic (10); these events are therefore extremely challenging to identify based on short read sequencing data of exonic regions and off-target reads.

10. Response and progression data

Radiological response to first- and second-line chemotherapy was defined using measured change in disease using bidirectional measurements: complete response was defined as complete resolution of pre-treatment disease, partial response (PR) was defined as disease reduction by ≥50%, progressive disease (PD) was defined as radiologically-confirmed appearance of new lesions or ≥50% increase in tumour size. Evaluable cases not reaching criteria for PR or PD were classified as stable disease (SD).

CA125 tumour marker response was evaluated using GCIG criteria (11): complete response (GCIG-CR); was defined as confirmed normalisation of CA125 after a pre-treatment baseline value at least twice the upper limit of normal; partial response (GCIG-50%) was defined as confirmed reduction of CA125 by at least 50% from a baseline value at least twice the upper limit of normal. CA125 progression was defined as confirmed doubling of CA125. Evaluable cases not reaching criteria for response or PD were classified as no change in CA125.

Progression-free survival (PFS) was defined as the time from pathologically confirmed diagnosis to first progression event (radiological PD, radiologically confirmed recurrence or CA125 progression by GCIG criteria). 32 cases were non-evaluable for PFS time due to insufficient investigations.

SUPPLEMENTARY TABLES

Supplementary Table S1. Identified mutations from targeted sequencing of 362 HGSOC cases

Gene	HGSOC cases with mutation	%
TP53	355	98.1
BRCA1	46	12.7
BRCA2	24	6.6
RB1	11	3.0
NF1	10	2.8
NF2, PIK3CA	8	2.2
CDK12	5	1.4
ARID1A	4	1.1
FANCA, KRAS, SLFN11, PER3, BRIP1	3	0.8
MSH6, CTNNB1, SLX4, CHEK2, PRKDC	2	0.6
CHD4, AC004223.3, PTEN, EMSY, FANCF, BRAF, PARP2, PAXIP1, ATM, CCNE1, RAD51C, BAP1, NBN, PALB2, FANCM, TP53BP1, GNAS, FANCC, RNASEH2B, PPP2R1A, MSH2, SLC25A40, ERCC4	1	0.3
ABCB1, ATR, ATRX, BARD1, BCL2L1, BLM, C11orf65, CHEK1, EGFR, ERBB2, EZH2, FANCB, FANCD2, FANCE, FANCG, FANCI, FANCL, KIT, MAD2L2, MDM2, MLH1, MRE11, MUS81, MUTYH, NDUFB2, NRAS, PARP1, PDGFRA, PMS2, PPP2R2A, RAD50, RAD51, RAD51B, RAD54L, RNASEH2A, RNASEH2C, RPA1, RUNDC3B, SHFM1, TOE1, UBE2T, VRK2	0	0.0

HGSOC, high grade serous ovarian carcinoma

Supplementary Table S2. Comparison of *EMSY* overexpression versus copy number status

	***EMSY* expression status**	
	Overexpressed	Wild-type
***EMSY* CN status**		
Amplified	10	14
Non-amplified	42	296
Chi-squared test P<0.001		

For amplification status as a predictor of overexpression: positive predictive value 0.42 (95% CI 0.22-0.63); negative predictive value 0.88 (95% CI 0.84-0.91); sensitivity 0.19 (95% CI 0.10-0.33); specificity 0.95 (95% CI 0.93-0.98)

Supplementary Table S3. Multivariable analysis of overall survival across HRR-centric subgroups

		mHR	95% CI	P-value
HRR-centric subtype	*BRCA1*m	0.88	0.61-1.27	0.500
	*BRCA2*m	0.40	0.25-0.64	<0.001
	*CCNE1*g	1.52	1.11-2.09	0.013
	high-*EMSY*	0.51	0.32-0.81	0.007
	HRRwt	ref	ref	ref
FIGO stage at diagnosis	I	0.48	0.23-0.99	0.049
	II	0.41	0.24-0.70	0.002
	III	ref	ref	ref
	IV	1.42	1.06-1.90	0.031
	Unknown	0.77	0.33-1.85	0.521
Age at diagnosis	Years	1.01	0.99-1.02	0.521

Stratified by residual disease status. mHR, multivariable hazard ratio; 95% CI, 95% confidence interval; HRR, homologous recombination DNA repair; *BRCA1*m, *BRCA1*-mutant; *BRCA2*m, *BRCA2*-mutant; *CCNE1*g, *CCNE1* copy number gain; high-*EMSY*, *EMSY* overexpression; HRRwt, non-*CCNE1*g HRR wild-type; ref, reference population.

Supplementary Table S4. Comparison of transcriptomic subtyping approaches

	Tothill subtype			
TCGA subtype	**C1**	**C2**	**C4**	**C5**
DIF (n=102)	5 (5%)	15 (15%)	71 (70%)	11 (11%)
IMR (n= 94)	12 (13%)	62 (66%)	18 (19%)	2 (2%)
MES (n=99)	88 (89%)	3 (4%)	1 (1%)	7 (7%)
PRO (n=67)	5 (7%)	0 (0%)	1 (1%)	61 (91%)

Supplementary Table S5. Rates of complete surgical resection across molecular subgroups

		MacroRD	Zero RD	Unknown RD	% Zero RD	P-value	Bonferroni-adjusted P-value
HRR-centric subtype	nBRCA-HRRm	4	2	0	33.3	0.0165[c]	0.066
	*BRCA1*m	29	12	5	29.3		
	*BRCA2*m	17	4	3	19.0		
	*CCNE1*g	40	10	3	20.0		
	EMSY	21	9	1	30.0		
	HRRwt	159	28	15	15.0		
Transcript-ional subtype	DIF	74	20	8	21.3	0.0034[d]	0.0134
	IMR	58	26	10	31.0		
	MES	83	11	5	11.7		
	PRO	55	8	4	12.7		
CD3+ infiltration	CD3-high[a]	210	43	16	17.0	0.0569	0.2275
	Reference[b]	55	22	10	28.6		
CD8+ infiltration	CD8-high[a]	213	39	17	15.5	0.0018	0.0072
	Reference[b]	55	26	9	32.1		

[a]infiltration burden within the top quartile; [b]infiltration burden within the lower three quartiles. [c]HRR-aberrant (*BRCA1*m, *BRCA2*m, *EMSY* overexpression or nBRCA-HRRm) vs HRRwt; [d] IMR vs other subtypes. MacroRD, macroscopic residual disease; Zero RD, complete macroscopic resection; HRR, homologous recombination DNA repair; nBRCA-HRRm, non-*BRCA1/2* HRR gene mutation; *BRCA1*m, *BRCA1*-mutant; *BRCA2*m, *BRCA2*-mutant; *CCNE1*g, *CCNE1* copy number gain; high-*EMSY*, *EMSY* overexpression; HRRwt, non-*CCNE1*g HRR wild-type.

SUPPLEMENTARY FIGURES

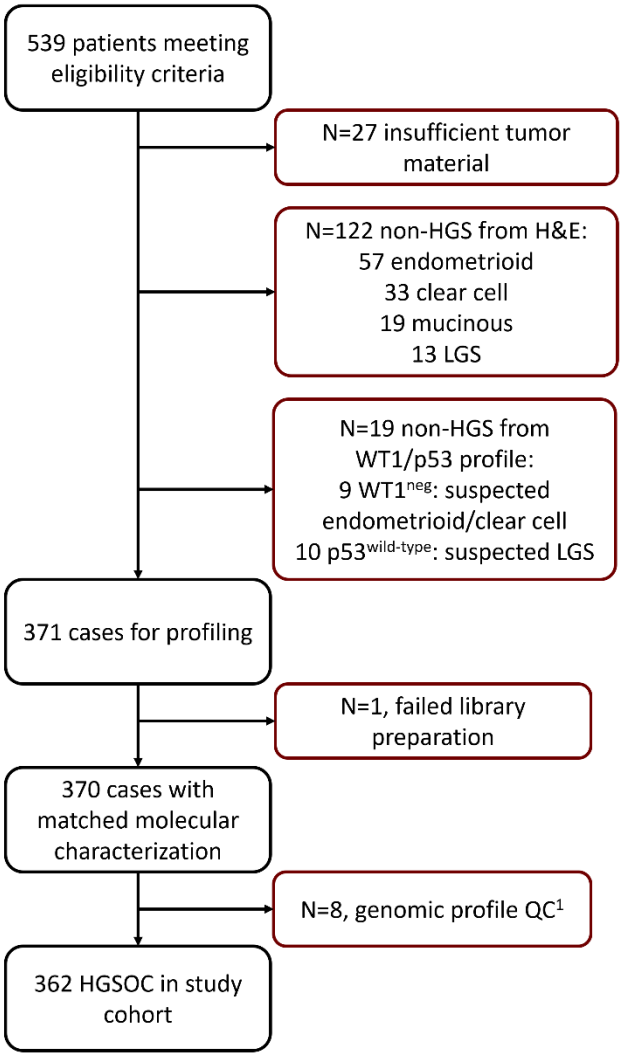

Figure S1. Case flow diagram for high grade serous ovarian carcinoma (HGSOC) cohort. [1]Excluded as likely non-HGS from genomic profile: *TP53* wild-type with mutation of *ARID1A*, *KRAS*, *PIK3CA* or *CTNNB1*. QC, quality control. LGS, low grade serous.

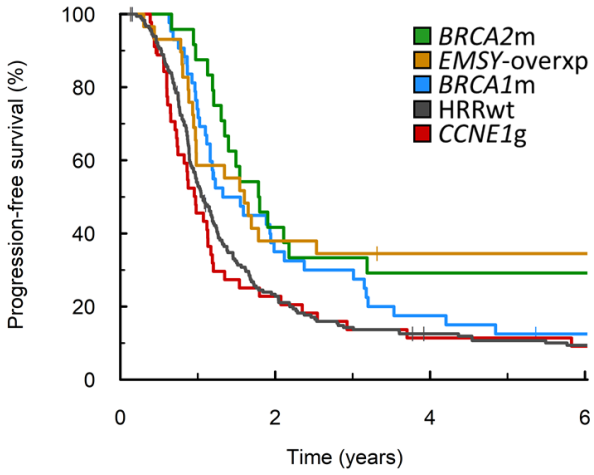

Figure S2. Progression-free survival of homologous recombination repair (HRR)-centric subtypes. *BRCA2*m, *BRCA2* mutant; *BRCA1*m, *BRCA1* mutant; *EMSY*-overxp; overexpression of *EMSY*; *CCNE1*g, gain of *CCNE1*; HRRwt, non-*CCNE1*g HRR wild-type.

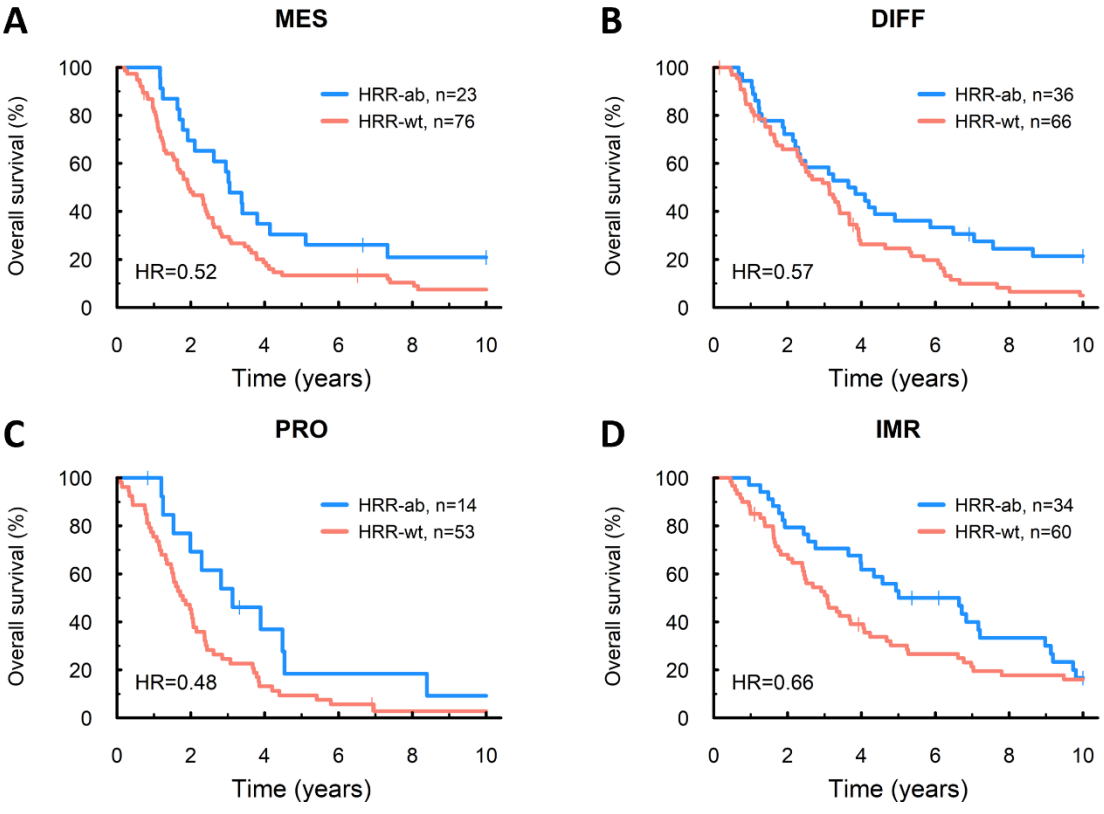

Figure S3. Impact of homologous recombination repair aberrations (HRR-aberrant: *BRCA1* mutation, *BRCA2* mutation, *EMSY*-overexpression or non-*BRCA* HRR gene mutation) on overall survival within TCGA transcriptomic subtypes. (A) Overall survival within the MES subtype. (B) Overall survival within the DIFF subtype. (C) Overall survival within the PRO subtype. (D) Overall survival within the IMR subtype. HRR-ab, HRR-aberrant; HRR-wt, HRR wild-type reference population: *CCNE1*-gained plus other HRR wild-type cases.

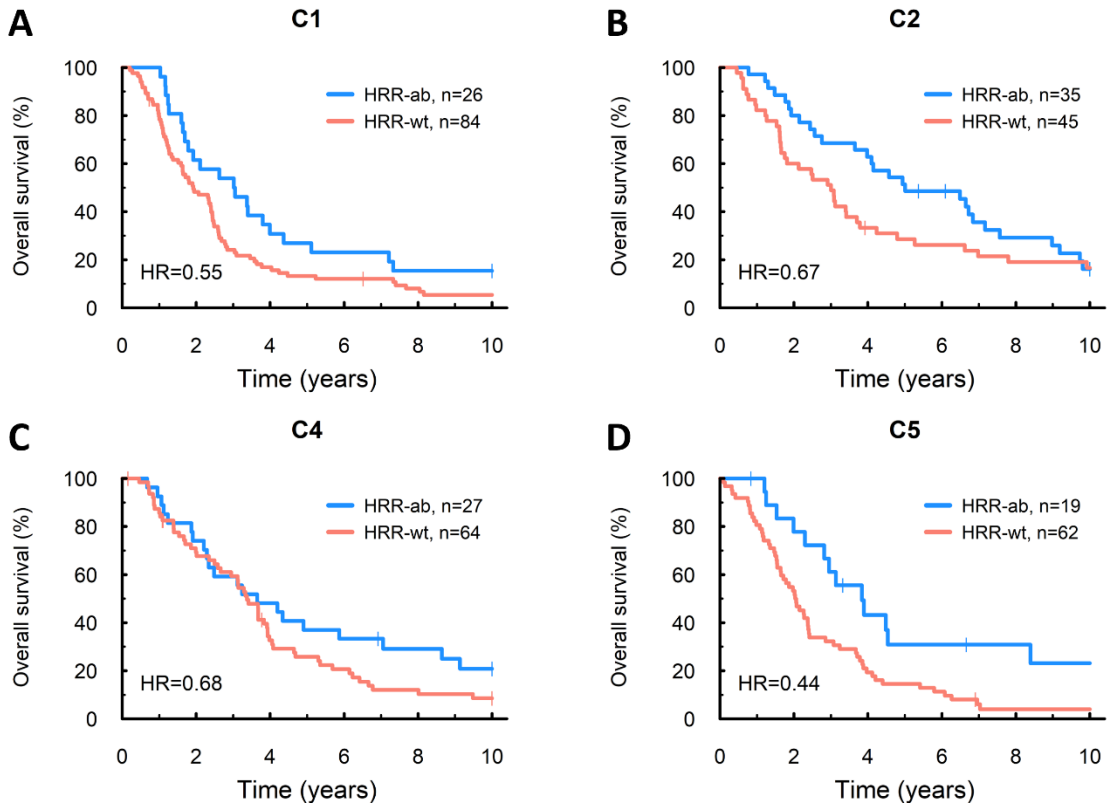

Figure S4. Impact of homologous recombination repair aberrations (HRR-aberrant: *BRCA1* mutation, *BRCA2* mutation, *EMSY*-overexpression or non-*BRCA* HRR gene mutation) on overall survival within Tothill transcriptomic subtypes. (A) Overall survival within the C1 subtype. (B) Overall survival within the C2 subtype. (C) Overall survival within the C4 subtype. (D) Overall survival within the C5 subtype. HRR-ab, HRR-aberrant; HRR-wt, HRR wild-type reference population: *CCNE1*-gained plus other HRR wild-type cases.

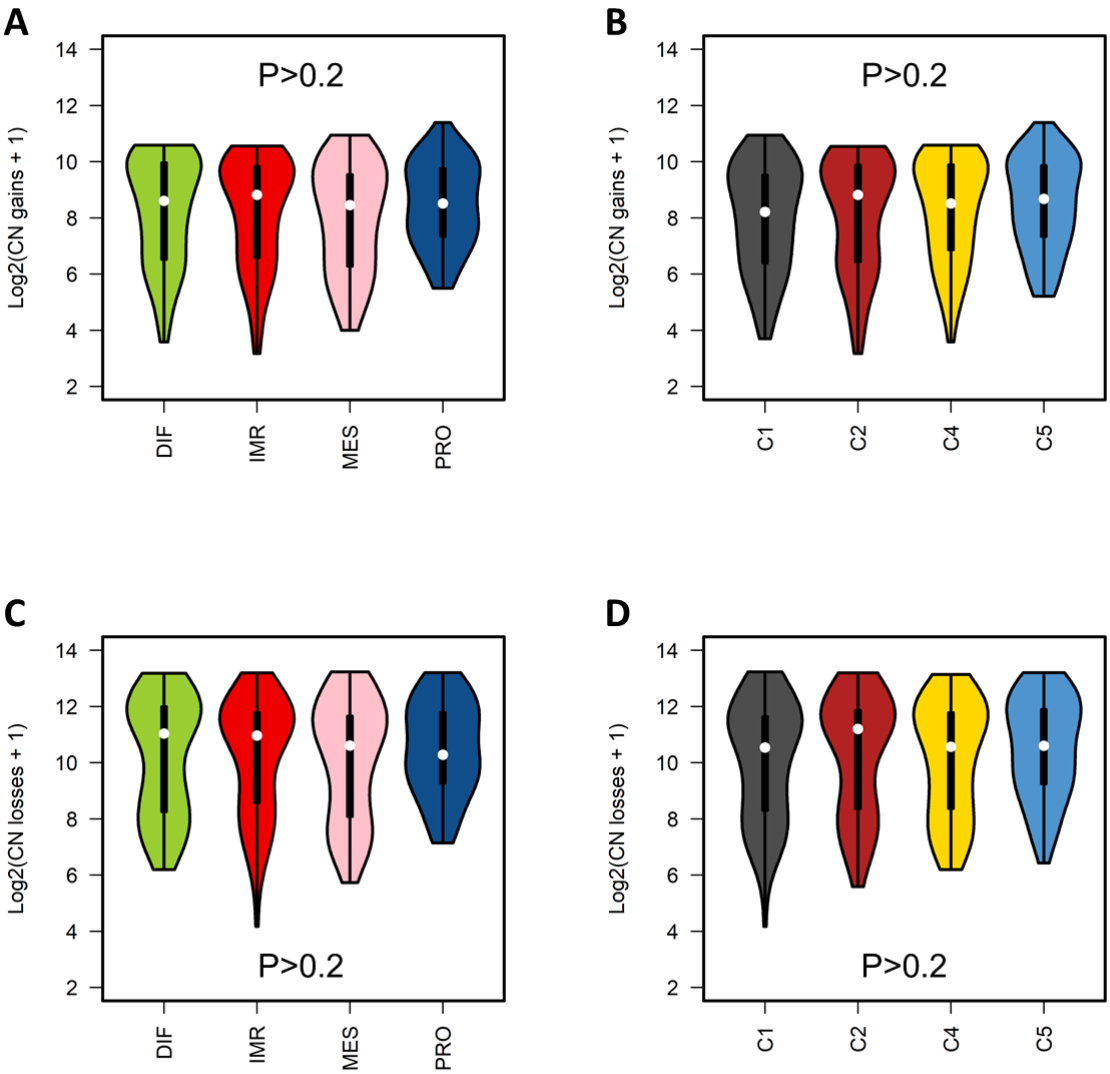

194

195 Figure S5. Violin plots of copy number (CN) gain and CN loss event burden across transcriptomic
196 subtypes of high grade serous ovarian carcinoma. (A) CN gain event burden across TCGA
197 transcriptomic subtypes. (B) CN gain event burden across Tothill transcriptomic subtypes. (C) CN loss
198 event burden across TCGA transcriptomic subtypes. (D) CN loss event burden across Tothill
199 transcriptomic subtypes.

200

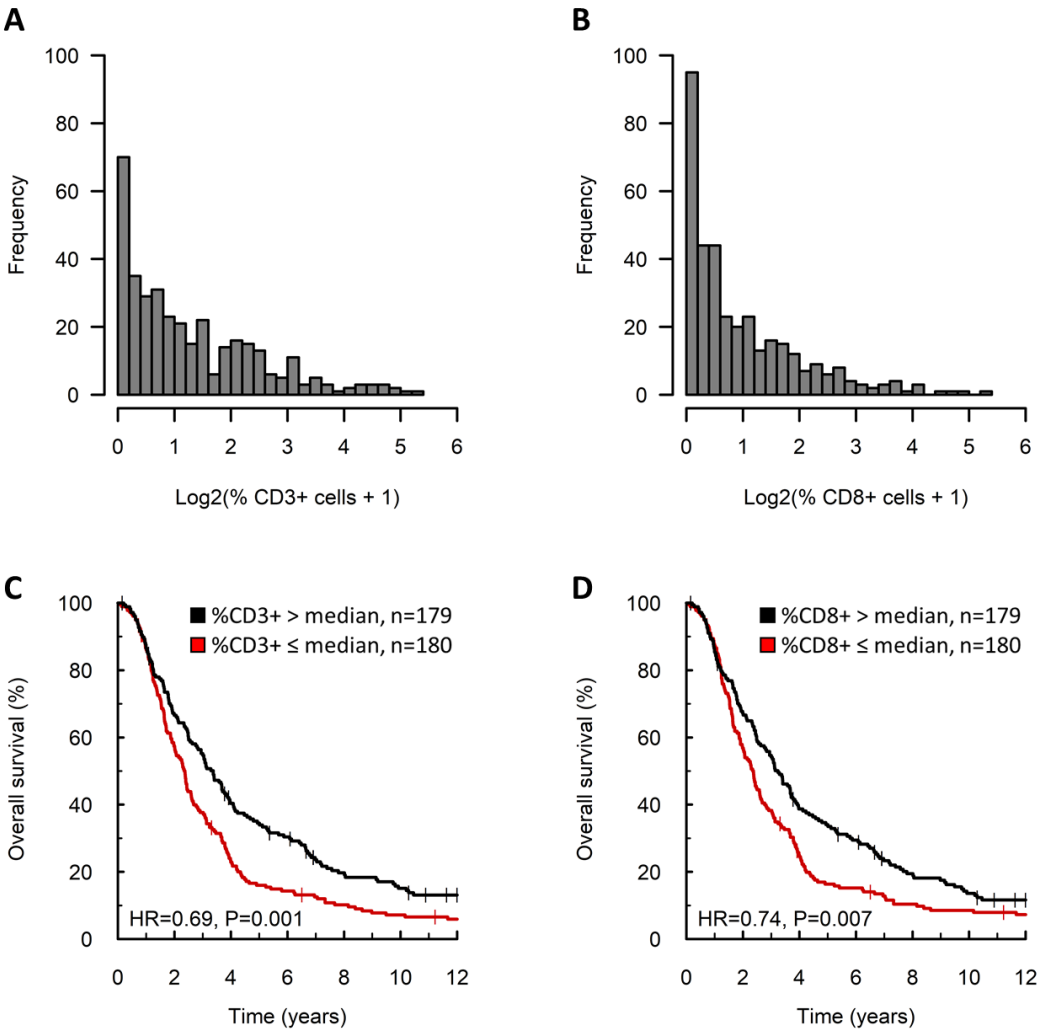

Figure S6. Tumour-infiltrating immune cells in high grade serous ovarian carcinoma. (A) Distribution of CD3+ infiltrating cell burden. (B) Distribution of CD8+ infiltrating cell burden. (C) Impact of CD3+ infiltrating cell burden on overall survival. (D) Impact of CD8+ infiltrating cell burden on overall survival.

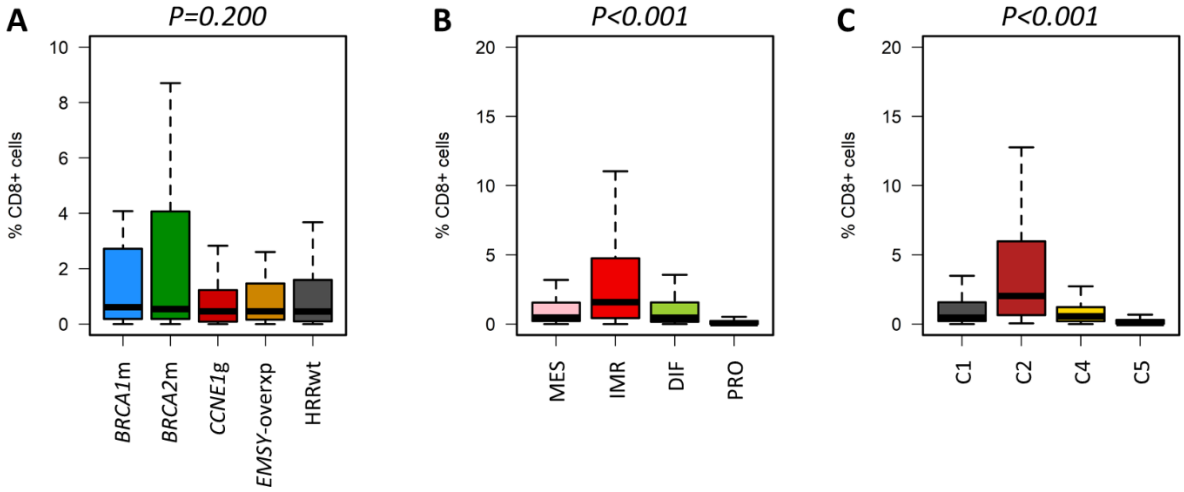

207

208 Figure S7. Tumour-infiltrating CD8+ cells across high grade serous ovarian carcinoma subtypes. (A)
209 CD8+ infiltration across HRR-centric subtypes; labelled P value represents comparison of *BRCA2*m and
210 *CCNE1*g groups using the Mann Whitney-U test. (B) CD8+ infiltration across TCGA transcriptomic
211 subtypes; labelled P value represents comparison of IMR and PRO groups using the Mann Whitney-U
212 test. (C) CD8+ infiltration across Tothill transcriptomic subtypes; labelled P value represents
213 comparison of C2 and C5 groups using the Mann Whitney-U test. *BRCA2*m, *BRCA2* mutant; *BRCA1*m,
214 *BRCA1* mutant; *EMSY*-overxp; overexpression of *EMSY*; *CCNE1*g, gain of *CCNE1*; HRRwt, non-*CCNE1*g
215 homologous recombination proficient.

216

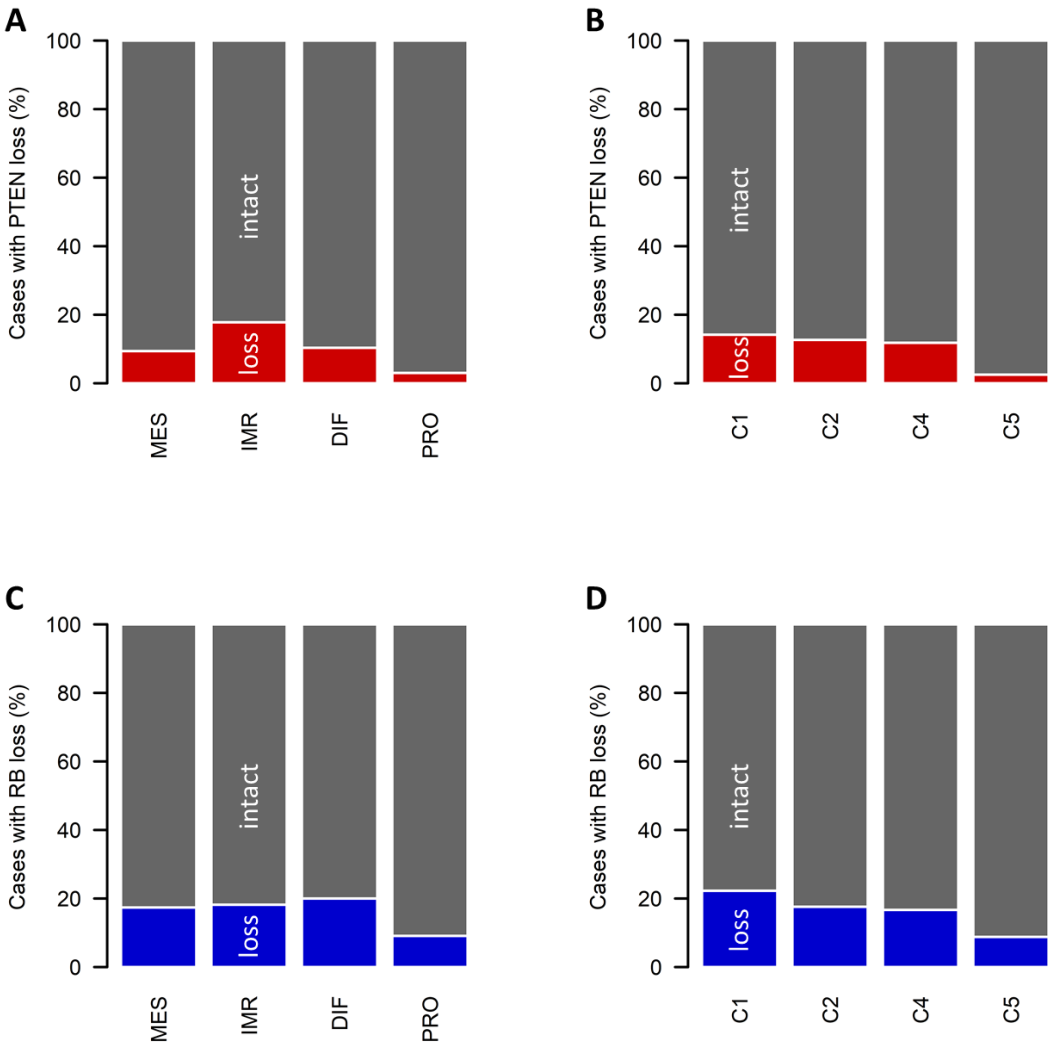

217

218 Figure S8. Loss of PTEN and RB protein expression across transcriptional subtypes of high grade serous
219 ovarian carcinoma. (A) PTEN loss across TCGA transcriptomic subtypes. (B) PTEN loss across Tothill
220 transcriptomic subtypes. (C) RB loss across TCGA transcriptomic subtypes. (D) RB loss across Tothill
221 transcriptomic subtypes.

222

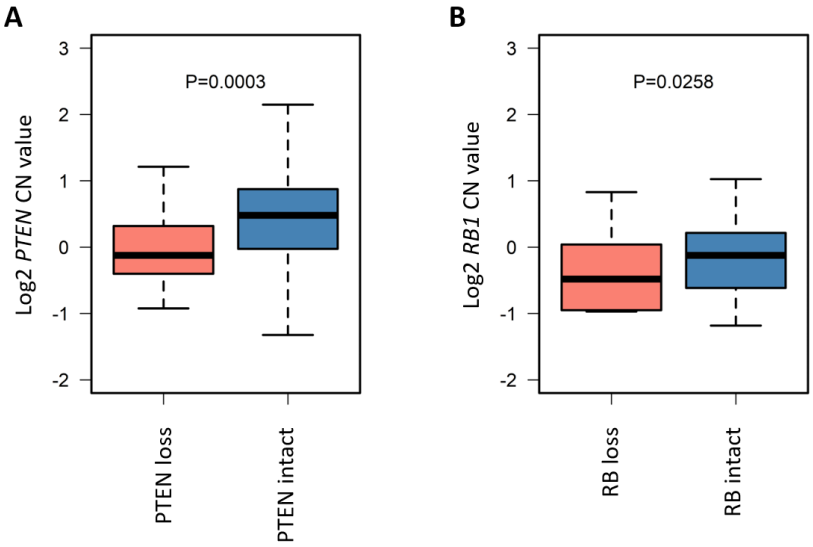

Figure S9. Calculated copy number (CN) of *PTEN* and *RB1* genes in cases with loss of PTEN and loss of RB expression, as determined by CopywriteR. (A) *PTEN* CN estimates between PTEN-lost and PTEN-intact cases. (B) *RB1* CN estimates between RB-lost and RB-intact cases.

Supplementary references

1. Gourley C, McCavigan A, Perren T, Paul J, Michie CO, Churchman M*, et al.* Molecular subgroup of high-grade serous ovarian cancer (HGSOC) as a predictor of outcome following bevacizumab. *Journal of Clinical Oncology* 2014;**32**(15_suppl):5502 doi 10.1200/jco.2014.32.15_suppl.5502.
2. Hollis RL, Churchman M, Michie CO, Rye T, Knight L, McCavigan A*, et al.* High EMSY expression defines a BRCA-like subgroup of high-grade serous ovarian carcinoma with prolonged survival and hypersensitivity to platinum. *Cancer* 2019;**125**(16):2772-81 doi 10.1002/cncr.32079.
3. Kobel M, Piskorz AM, Lee S, Lui S, LePage C, Marass F*, et al.* Optimized p53 immunohistochemistry is an accurate predictor of TP53 mutation in ovarian carcinoma. *The journal of pathology Clinical research* 2016;**2**(4):247-58 doi 10.1002/cjp2.53.
4. Garrison E, Marth G. Haplotype-based variant detection from short-read sequencing. *arXiv preprint* 2012;**arXiv:1207.3907 [q-bio.GN]**.
5. Lai Z, Markovets A, Ahdesmaki M, Chapman B, Hofmann O, McEwen R*, et al.* VarDict: a novel and versatile variant caller for next-generation sequencing in cancer research. *Nucleic acids research* 2016;**44**(11):e108 doi 10.1093/nar/gkw227.
6. Cibulskis K, Lawrence MS, Carter SL, Sivachenko A, Jaffe D, Sougnez C*, et al.* Sensitive detection of somatic point mutations in impure and heterogeneous cancer samples. *Nature biotechnology* 2013;**31**(3):213-9 doi 10.1038/nbt.2514.
7. Landrum MJ, Lee JM, Riley GR, Jang W, Rubinstein WS, Church DM*, et al.* ClinVar: public archive of relationships among sequence variation and human phenotype. *Nucleic acids research* 2014;**42**(Database issue):D980-5 doi 10.1093/nar/gkt1113.
8. Chen GM, Kannan L, Geistlinger L, Kofia V, Safikhani Z, Gendoo DMA*, et al.* Consensus on Molecular Subtypes of High-Grade Serous Ovarian Carcinoma. *Clinical cancer research : an official journal of the American Association for Cancer Research* 2018;**24**(20):5037-47 doi 10.1158/1078-0432.Ccr-18-0784.
9. Kuilman T, Velds A, Kemper K, Ranzani M, Bombardelli L, Hoogstraat M*, et al.* CopywriteR: DNA copy number detection from off-target sequence data. *Genome biology* 2015;**16**(1):49 doi 10.1186/s13059-015-0617-1.
10. van Belzen I, Schönhuth A, Kemmeren P, Hehir-Kwa JY. Structural variant detection in cancer genomes: computational challenges and perspectives for precision oncology. *NPJ Precis Oncol* 2021;**5**(1):15 doi 10.1038/s41698-021-00155-6.
11. Rustin GJ, Vergote I, Eisenhauer E, Pujade-Lauraine E, Quinn M, Thigpen T*, et al.* Definitions for response and progression in ovarian cancer clinical trials incorporating RECIST 1.1 and CA 125 agreed by the Gynecological Cancer Intergroup (GCIG). *International journal of gynecological cancer : official journal of the International Gynecological Cancer Society* 2011;**21**(2):419-23 doi 10.1097/IGC.0b013e3182070f17.